INTERNATIONAL JOURNAL FOR NUMERICAL METHODS IN FLUIDS
Int. J. Numer. Meth. Fluids 2009; **59**:285–307
Published online 16 January 2007 in Wiley InterScience (www.interscience.wiley.com). DOI: 10.1002/fld.1419

Some recent numerical advances for two-phase flow modelling in NEPTUNE project

J. M. Hérard[1,*,†] and O. Hurisse[2]

[1]*EDF-Recherche Développement, Département MFEE, 6 quai Watier, Chatou 78400, France*
[2]*CMI-LATP, UMR CNRS 6632, 39 rue Joliot Curie, Marseille 13453, France*

SUMMARY

This paper is devoted to a brief review of some problems arising in the NEPTUNE project, whose main objective consists in preparing a new generation of two-phase flow codes covering the whole range of modelling scales for nuclear power plants. Focus is given on multi-phase flow modelling and on the unsteady coupling of existing codes. Some recent results are displayed and a few open problems are discussed in the manuscript. A draft version of this paper has been presented as an invited lecture during the FVCA4 meeting. Copyright © 2007 John Wiley & Sons, Ltd.

Received 9 May 2006; Revised 9 November 2006; Accepted 10 November 2006

KEY WORDS: finite volumes; multi-phase flows; coupling methods

1. INTRODUCTION

The NEPTUNE Project gathers some of the efforts of CEA and EDF in terms of Research and Development programs (see [1]). It aims at building the next generation of water–vapour two-phase flow codes for nuclear energy applications. It should allow real-time simulation using the system scale, but also perform multi-scale three-dimensional computations. Three main work packages

*Correspondence to: J. M. Hérard, EDF-Recherche Développement, Département Mécanique des Fluides Energies et Environment, 6 quai Watier, Chatou 78400, France.
†E-mail: Jean-Marc.Herard@edf.fr

Contract/grant sponsor: Electricité de France
Contract/grant sponsor: Commissariat à l'Energie Atomique
Contract/grant sponsor: Institut de Radioprotection et Sureté Nucléaire
Contract/grant sponsor: AREVA-NP

arise:

- A first one is dedicated to software development.
- A second one benefits from physical investigations [2] and numerical research investigations.
- A third one is devoted to two-phase flow metrology, physical experiments and advanced instrumentation techniques [3].

The paper [1] gives a precise review of the whole project including software developments, and the reader is also referred to [2, 3] for additional information.

Numerical methods are obviously part of the long-term research programme, and should not only support software developers, but also provide new ideas and methods to improve our understanding of multi-phase flows. This paper intends to describe some of these. Actually, some of the numerical problems arising in the NEPTUNE project concern the establishment of sets of partial differential equations which may account in an expected meaningful and relevant way for multi-phase flows. The second main issue concerns the numerical simulation of these systems, including the coupling of new or existing codes.

Though finite volume methods [4] are the keystone of almost all NEPTUNE developments, some methods rely on the use of finite element approach, or alternatively on the finite volume element approach. In Section 2, we will give a very brief overview of some recent achievements in numerical methods. Then we will focus on the modelling of multiphase flows in Section 3. In Section 4, we will discuss some open questions and recent advances related to the unsteady coupling of codes in a finite volume framework.

2. A BRIEF REVIEW OF SOME CURRENT NUMERICAL ACTIVITIES

2.1. Direct numerical simulation of two-phase flows

First, we would like to mention the original work on the modelling of interfaces reported in [5–10]. It is grounded on an original approach which is consistent with thermodynamical concepts. The mean density, the liquid mass fraction, the mean velocity, the local pressure and the position of the interface are computed with help of a five-equation hyperbolic model, which possess a quasi-conservative form. Suitable upwinding techniques are used to provide approximations of solutions on colocated meshes. This work not only examines the problem of the handling of pure convective effects, but it also investigates the closure and the approximation of interfacial mass transfer, which is achieved in agreement with an entropy inequality. This approach is clearly related to the direct numerical simulation strategy, and aims at getting rid of any averaging process, in order to provide a precise prediction of the local behaviour in some extreme situations, including the boiling crisis topic. We refer to the papers mentioned above which provide a detailed investigation of the topics.

2.2. Finite volume approximations of standard two-fluid models

A second contribution concerns the numerical approximation of standard two-fluid models, which rely on the single-pressure assumption. The six governing equations for these two-fluid models correspond to the mass balance equations, the momentum equations and the total energy balance equations within each phase. This approach is rather widespread, at least when one focuses on gas–particle flows. It requires to develop codes in order to compute approximations of solutions of

DOI: 10.1002/fld

sets of equations, the convective part of which is not necessarily hyperbolic. These models usually contain some modifications of momentum equations, which contribute to enlarge the hyperbolicity domain. Another specific feature is that these sets of partial differential equation (PDE) include first-order non-conservative contributions, which render their numerical simulation rather tricky. Thus, the use of well-known approximate Riemann solvers, such as the Roe scheme, cannot be straightforward, and requires to specify modifications in order to account for possible entrance in 'time-elliptic regions', but also to cope with non-conservative contributions. Some numerical strategies involving finite volume approximations on unstructured meshes have been proposed quite recently, and a great effort is done in order to validate the whole approach, while including refined physical models such as the MUSIG (multisize group) model for instance (see among others [11–13]).

2.3. Numerical algorithms to account for complex equations of state

Another contribution has been devoted to the numerical approximation of homogeneous two-phase flow models. Owing to the fact that we deal with nuclear applications in pressurized power reactors, there is an urgent need for specific algorithms to compute Euler-type models with complex equation of state (EOS). Actually, water–vapour tabulations require that one might compute complex EOS in homogeneous codes. The work [14] precisely suggests some unified framework to achieve that. It shows that some classes of EOS enable the use of suitable interface Riemann solvers, while retaining the standard conservative approach for mass, momentum and energy balances. Besides, it details how to cope with other EOS which do not belong to the latter class, in order to maintain particular patterns such as moving contact discontinuities, by computing a modified discrete pressure field. It also clearly indicates whether one may expect to obtain convergence towards the true shock solution or not, depending on the class of EOS. It eventually suggests hybrid techniques in order to ensure convergence towards the correct solution, when shocks and contact discontinuities are present in the solution, while achieving a reasonable error on coarse meshes in any case.

2.4. Computation of low Mach number flows

Once again, the mean flow in standard situations in the nuclear power plant coolant circuit looks like a single-phase water flow. Thus, the local Mach number is small, and therefore conservative upwinding approximate Riemann solvers sometimes lead to a poor accuracy on coarse meshes. This has motivated the development of preconditioning techniques for low Mach number applications, which are indeed useful for practical steady situations (see [15]). Besides, the standard problem of linear algebra preconditioning still needs to be addressed, especially for the GENEPI code and other codes which rely on classical projection techniques (see [16–18]).

2.5. Fictitious domain methods and other techniques

Another important contribution [19], which addresses the capabilities of finite volume element techniques to handle accurate approximations of two-fluid models, is based on the early contribution [20] which focused on Navier–Stokes equations. Another research direction pertains to the use of fictitious domain methods, which might represent an alternative accurate way to account for complex geometries, on the basis of simple structured codes (see [21–26]). The last research domain concerns the improvement of unstructured finite volume codes on colocated meshes [27].

DOI: 10.1002/fld

We now will focus on the modelling of multi-phase flows and afterwards on the interfacial coupling of unsteady codes.

3. NUMERICAL MODELLING OF MULTI-PHASE FLOWS

3.1. Simulation of two-fluid models

One of the main problems arising in the numerical modelling of two-phase flows is that sets of PDE which are expected to represent main patterns of such flows are still not clearly identified or may suffer from severe drawbacks. This is particularly clear when focusing on the so-called two-fluid approach. Associated six-equation single-pressure models account for mass conservation, momentum and total phase energy balance within each phase. Everyone is aware of the potential loss of hyperbolicity of standard single-pressure two-fluid models in some areas, which unfortunately may easily arise, even for (expected so) simple sets of initial values, such as those described in [28]. This main drawback seems to be closely linked with the assumption of local instantaneous pressure equilibrium. It seems that the blow up of codes may be quite easily postponed when applying for upwinding techniques, and restricting to coarse meshes. Nonetheless, even when drag effects are accounted for, it may be easily checked that the inner stabilization of the latter schemes is no longer sufficient on very fine meshes (see [29], for instance).

This has led some workers to reexamine 'father' models known as two-fluid two-pressure models, following the pioneering work of Baer and Nunziato [30], Kapila *et al.* [31], Gavrilyuk *et al.* [32], Gavrilyuk and Gouin [33]. These benefit from classical properties, in the sense that: (i) the convective subset is hyperbolic for any physically relevant choice of the state variable; (ii) the whole set may be controlled by an entropy inequality for regular solutions, which meets agreement with true source terms and viscous terms. Under the constraint: $\alpha_1 + \alpha_2 = 1$, the basic form of the governing set of equations is the following (for $k = 1, 2$):

$$\frac{\partial \alpha_k}{\partial t} + U_I \frac{\partial \alpha_k}{\partial x} = \lambda (P_k - P_{3-k})(P_k + P_{3-k})^{-1} \tag{1}$$

$$\frac{\partial \alpha_k \rho_k}{\partial t} + \frac{\partial \alpha_k \rho_k U_k}{\partial x} = 0 \tag{2}$$

$$\frac{\partial \alpha_k \rho_k U_k}{\partial t} + \frac{\partial \alpha_k (\rho_k (U_k)^2 + P_k)}{\partial x} - P_I \frac{\partial \alpha_k}{\partial x} = -\mu (m_k m_{3-k})^{1/2} (U_k - U_{3-k}) \tag{3}$$

$$\frac{\partial (\alpha_k E_k)}{\partial t} + \frac{\partial (\alpha_k U_k (E_k + P_k))}{\partial x} + P_I \frac{\partial \alpha_k}{\partial t} = -\mu (m_k m_{3-k})^{1/2} U_I (U_k - U_{3-k}) \tag{4}$$

Where α_k, ρ_k, $m_k = \alpha_k \rho_k$, U_k, $E_k = \rho_k e_k(\rho_k, P_k) + \rho_k U_k^2/2$, $e_k(\rho_k, Pk)$ and P_k, respectively, stand for the void fraction, the mean density, the partial mass, the mean velocity, the total energy, the internal energy and the local pressure within phase k (for $k = 1, 2$). The problem of the closure of non-conservative products may even be circumvented for some specific choices of the interfacial velocity U_I and of the interfacial pressure P_I (see [34]). If we set

$$U_\mathrm{I} = \beta U_1 + (1 - \beta) U_2 \tag{5}$$

DOI: 10.1002/fld

we know that admissible forms of the interfacial velocity are $U_I = U_1$ or $U_I = U_2$ or alternatively:

$$U_I = \frac{(m_1 U_1 + m_2 U_2)}{(m_1 + m_2)} \tag{6}$$

The latter three correspond to $\beta = 1$, $\beta = 0$, and $\beta = m_1/(m_1 + m_2)$. Hence, the correct definition of P_I will be

$$P_I = \mu P_1 + (1 - \mu) P_2$$

with

$$\mu = a_1(1 - \beta)/(a_1(1 - \beta) + a_2\beta) \tag{7}$$

and

$$a_k = \frac{\partial \operatorname{Log}(s_k(\rho_k, P_k))}{\partial P_k} \Big/ \frac{\partial e_k(\rho_k, P_k)}{\partial P_k} \tag{8}$$

One or two-equation turbulence closures may be included, without breaking the keen wave structure (see, for instance, [35–37]). We, however, emphasize that the problem of existence and uniqueness of the solution of the 1D Riemann problem is still an open topic, mainly due to the great complexity of the wave structure, and to the possible resonance phenomenon, which seems to forbid uniqueness of solutions, unless some consistent criteria is added. Some preliminary results are available in [34, 38].

Straightforward upwinding techniques can be easily implemented, which provide reasonable numerical results (see [34]). Among these, both the Rusanov scheme and the approximate Godunov schemes introduced in [39] have been examined. Other numerical techniques have been recently proposed (see [40]). An essential point to quote is that converged solutions do not depend on schemes though non-conservative products are present in the governing equations for mass, momentum and energy. This point is clearly examined in [41]. Due to the (six or) seven distinct eigenvalues, some of them being close to one another, intermediate states in the solution of the 1D Riemann problem can hardly be distinguished in some situations, unless one considers a huge mesh refinement, which can hardly be afforded when turning to 3D flow simulations.

Another problem immediately occurs in this framework: is there some way to deal with both standard single-pressure two-fluid models and these two-pressure hyperbolic models? Based on recent work pertaining to relaxation methods, the temptation is great to take advantage of the 'father–son' structure of the couple of models. Following [7, 42–44], one may for instance compute the six-equation single-pressure model considering two steps as follows:

(i) a first evolution step, which computes some approximation of solutions of the IVP problem connected with the hyperbolic seven-equation two-pressure model,
(ii) an instantaneous relaxation step which locally equilibrates both pressure fields at the end of each time step.

Obviously, the input of (i) is the output of (ii), which guarantees a pressure equilibrium. The HAT (hybrid alternative tool) algorithm enjoys rather interesting properties. The whole scheme identifies with the one in [34], when the inverse of the pressure relaxation time λ remains bounded. The spirit is almost the same as the one from [28], and we also underline that the numerical treatment of step (ii) is exactly the same, and provides consistent approximations of the mean pressure field.

DOI: 10.1002/fld

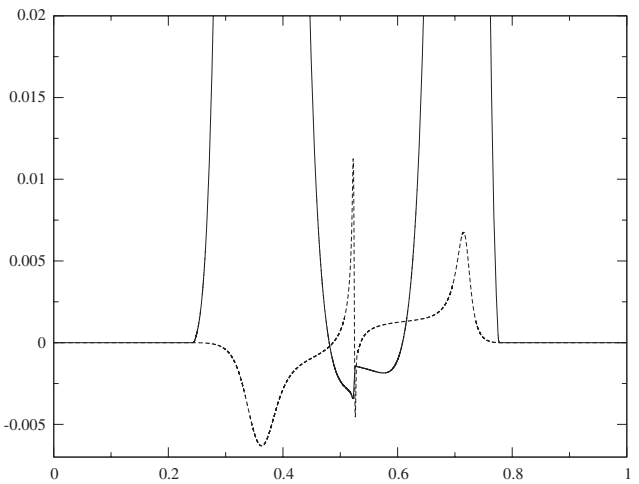

Figure 1. Relative velocity U_r (plain line) and a translation of the void fraction profile $(\alpha_1 - \alpha_1(x, t=0))$ (dashed line) when computing approximations of solutions, using the initial value problem given in [28]. On the basis of the two-pressure approach, the relaxation technique enables to compute approximations of the two-fluid single-pressure model which accounts for drag source terms. The bubble diameter is equal to $d = 10^{-3}$. The present mesh contains 250 000 cells.

It might represent some possible way to tune models through the next coming years (see [45]). It also seems an appealing way to provide meaningful boundary conditions in six-equation two-fluid models.

Results: We show in [37] some approximations of the solution of a Riemann problem using a turbulent closure within each phase. The structure of the density fields, the velocity fields, and the modified pressure fields ($\pi_k = P_k + 2K_k/3$) is displayed. One may also refer to [37] which examines from a practical point of view the influence of the couple (U_I, P_I) on the computational results on very fine grids (and thus the true influence of this closure). This is quite interesting due to the fact that some authors might prefer to use one specific closure.

Figure 1 shows the behaviour of the void fraction $(\alpha_1 - 0.25)$ when computing approximate solutions of a standard two-fluid model with a relaxation method on a very fine mesh (250 000 cells). This latter result issues from [29]. The initial conditions are the following (see [28]):

$$
\begin{aligned}
&U_1(x, t=0) = U_2(x, t=0) = 0\\
&\alpha_1(x, t=0) = 0.25\\
&h_1(x, t=0) = 3.093 \times 10^6\\
&P(x<0.5, t=0) = 2 \times 10^7 \quad \text{and} \quad P(x>0.5, t=0) = 1.5 \times 10^7\\
&h_2(x<0.5, t=0) = 1.35 \times 10^6 \quad \text{and} \quad h_2(x>0.5, t=0) = 2.35 \times 10^6
\end{aligned}
\tag{9}
$$

DOI: 10.1002/fld

Though a Rusanov scheme has been used to compute convective fluxes, which ensures that the discrete cell values of the void fraction α_1 remain positive and smaller than 1, the code blows up on a finer mesh including 400 000 cells, due to the occurrence of a non-zero imaginary part in eigenvalues. This means that the relaxation procedure is able to retrieve structural deficiencies of the standard two-fluid model, when it enters a time-elliptic region that renders the initial value problem ill posed. Similar numerical experiments with a far less diffusive scheme such as the one introduced in [39] lead to a blow up on coarser grids (see [41]).

3.2. A new class of hyperbolic three-field models

Some specific applications in the nuclear energy require considering a mixture of liquid droplets in a continuum of vapour surrounded by a continuous liquid phase. The expected velocity of droplets inside the gas phase is clearly different from the local gas velocity. This is referred to as a three-field pattern in the nuclear community, and emerging ideas seem to retain an alternative way to tackle this problem, which consists in the modelling of three-phase flows. We may choose this approach, but a straightforward consequence is that the potential lack of hyperbolicity obviously arises once more. An obvious idea is to mimic the two-fluid approach discussed above, and thus constructing hyperbolic three-phase models. A first attempt is sketched in [46], the basics of which are recalled below. Using obvious notations, the governing set of equations reads:

$$\alpha_1 + \alpha_2 + \alpha_3 = 1 \tag{10}$$

$$\frac{\partial \alpha_k}{\partial t} + U_{\mathrm{I}} \frac{\partial \alpha_k}{\partial x} = \phi_k \tag{11}$$

$$\frac{\partial \alpha_k \rho_k}{\partial t} + \frac{\partial \alpha_k \rho_k U_k}{\partial x} = 0 \tag{12}$$

$$\frac{\partial \alpha_k \rho_k U_k}{\partial t} + \frac{\partial \alpha_k (\rho_k U_k^2 + P_k)}{\partial x} + \sum_{l=1, l\neq k}^{3} P_{kl} \frac{\partial \alpha_l}{\partial x} = S_{U_k} \tag{13}$$

$$\frac{\partial \alpha_k E_k}{\partial t} + \frac{\partial \alpha_k U_k (E_k + P_k)}{\partial x} - \sum_{l=1, l\neq k}^{3} P_{kl} \frac{\partial \alpha_l}{\partial t} = U_{\mathrm{I}} S_{U_k} \tag{14}$$

together with: $E_k = \rho_k e_k(\rho_k, P_k) + \rho_k U_k^2/2$. The momentum interfacial transfer terms cancel when being summed up, thus:

$$S_{U_1}(W) + S_{U_2}(W) + S_{U_3}(W) = 0 \tag{15}$$

A similar remark holds for unknown functions ϕ_k:

$$\phi_1 + \phi_2 + \phi_3 = 0 \tag{16}$$

and for P_{kl} contributions:

$$P_{12} + P_{32} = P_{13} + P_{23} = P_{21} + P_{31} \tag{17}$$

DOI: 10.1002/fld

If one focuses on the counterpart of the Baer–Nunziato model, thus setting $U_I = U_1$, this will result in the unique choice:

$$P_{13} = P_{31} = P_{32} = P_3 \tag{18}$$

$$P_{12} = P_{21} = P_{23} = P_2 \tag{19}$$

and therefore:

$$S_{U_k}(W) = m_k \psi_k(W)(U_1 - U_k) \tag{20}$$

for $k = 2, 3$, assuming positive values for $\psi_k(W)$, but also:

$$\phi_2 = \alpha_2(f_{1-2}(W)\alpha_1(P_2 - P_1) + f_{2-3}(W)\alpha_3(P_2 - P_3))/(|P_1| + |P_2| + |P_3|) \tag{21}$$

$$\phi_3 = \alpha_3(f_{1-3}(W)\alpha_1(P_3 - P_1) + f_{2-3}(W)\alpha_2(P_3 - P_2))/(|P_1| + |P_2| + |P_3|) \tag{22}$$

The frequencies $f_{k-l}(W)$ should remain bounded. As occurs when focusing on two-phase flows, the closure $U_I = U_1$ provides a meaningful framework in terms of closure of non-conservative products. This is due to the fact that the field corresponding to $\lambda = U_I$ turns to be a linearly degenerated field when defining $U_I = U_1$. One can note that in this particular case, the model looks like the counterpart of the Baer–Nunziatto model [30].

Moreover, the average 'mixture' velocity:

$$U_I = \frac{\sum_k (m_k U_k)}{\sum_k (m_k)} \tag{23}$$

also makes sense in this particular framework, as soon as P_{kl} interface pressures are adapted in consequence (see [46]). This extends in a straightforward way results of [34, 47].

We eventually emphasize that admissible forms of interfacial mass, energy and momentum transfer terms—that is forms which are consistent with the overall entropy inequality—slightly differ from the two-phase counterpart (see [48]). The whole approach provides a hyperbolic framework to tackle three-phase flows, and the results seem to confirm that the resonance phenomena is the only barrier remaining before solving the one dimensional Riemann problem. This first attempt obviously requires deeper investigations.

This approach can also be useful to compute approximations of single-pressure models with help of relaxation techniques, at least when EOS are simple enough, and of course restricting to coarse enough meshes (see [29]).

Results: We show in Figure 2 the structure of the pressure fields when computing a Riemann problem, while neglecting drag terms. We use here a mesh with 10^4 regular cells to describe the computational domain $[-0.5, 0.5]$. The time step is in agreement with the Courant–Friedrichs–Lewy (CFL) condition CFL = 0.49. The three phases are at rest and share the same pressure on

DOI: 10.1002/fld

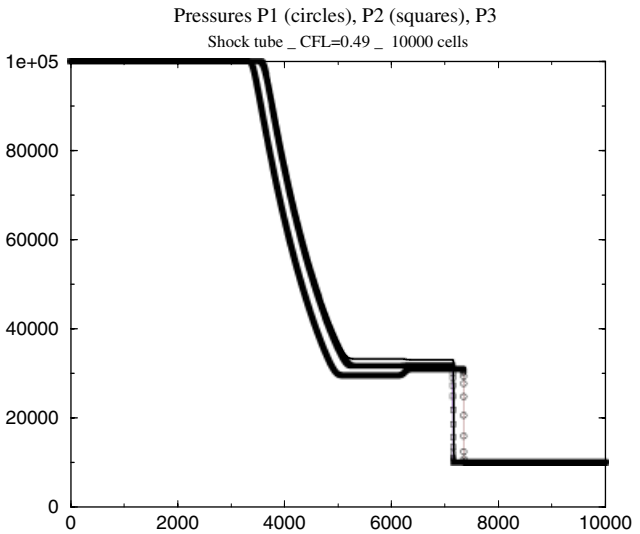

Figure 2. Behaviour of P_1, P_2, P_3 when computing a standard Riemann problem (hyperbolic three-phase flow model), using the interface velocity $U_I = U_1$. The three pressures vary through the contact discontinuity $\lambda = U_1$ which supports the unique void fraction discontinuity. The mesh contains 10 000 cells, and the domain is $[-0.5, 0.5]$. A non-conservative version of the Rusanov scheme was used for this test case. The CFL number has been set to 0.49.

each side of the membrane before the beginning of the computation:

$$\begin{aligned}
U_1(x, t=0) &= U_2(x, t=0) = U_3(x, t=0) = 0 \\
\alpha_1(x, t=0) &= 0.25 \\
P_1(x<0, t=0) &= P_2(x<0, t=0) = P_3(x<0, t=0) = 10^5 \\
P_1(x>0, t=0) &= P_2(x>0, t=0) = P_3(x>0, t=0) = 10^4 \\
\alpha_2(x<0, t=0) &= 0.4 \quad \text{and} \quad \alpha_3(x<0, t=0) = 0.5 \\
\alpha_2(x>0, t=0) &= 0.5 \quad \text{and} \quad \alpha_3(x>0, t=0) = 0.4 \\
\rho_1(x<0, t=0) &= \rho_2(x<0, t=0) = \rho_3(x<0, t=0) = 1 \\
\rho_1(x>0, t=0) &= \rho_2(x>0, t=0) = \rho_3(x>0, t=0) = 0.125
\end{aligned} \tag{24}$$

EOS in each phase correspond to perfect gas EOS, where $\gamma_1 = \frac{7}{5}$, $\gamma_2 = 1.005$, $\gamma_3 = 1.001$. One can note that all pressures vary through the contact wave associated with $\lambda = U_1$, as expected (see [46, 48]). Once again, the great number of intermediate states urges the need for very accurate solvers in order to perform computations on rather coarse meshes.

DOI: 10.1002/fld

4. THE COUPLING OF UNSTEADY CODES

There is nowadays a true need for coupling techniques in order to cope with industrial applications using current codes. This occurs for instance when computing the whole primary coolant circuit of the pressurized power reactor with help of different codes, for instance 3D codes (such as FLICA IV, THYC, etc.), which rely on the homogeneous approach to describe the core, and 1D codes (such as CATHARE, etc.), which apply for the standard two-fluid approach to describe patterns in pipes. No tools have been prepared for that purpose over the last years, and some simple—even steady—simulations which require some coupling have already exhibited major deficiencies. The NEPTUNE project team has decided to give special emphasis on that topic. It is also expected that this work will also contribute to extend our understanding of sole systems.

The main goal is to cope with the interfacial coupling of the system scale, the component scale and the local 3D computational fluid dynamics (CFD) scale. The basic strategy up to now consists in decoupling all effects, and then focusing on specific problems. We refer to [49] which synthesizes the needs, basic ideas and elementary tools available from the literature, whenever one considers the scalar case or the system case (see [50, 51]). We rather quickly detail below some of the recent achievements in that work package, and some ongoing work. The reader is invited to read [52–54] and related papers. A first attempt to couple a two-fluid model and an homogeneous model is described in [55].

4.1. Well-balanced schemes versus fractional step methods

Multi-phase CFD codes provide approximations of PDE which basically rely on contributions which account for convective effects and source terms (mass, energy and momentum interfacial transfer). The coupling of two codes will thus involve two sets of PDEs with different time scales (time scales associated with flashing phenomena, condensation or drag effects are indeed quite different!). Even before achieving any coupling, one may obviously wonder how numerical methods will deal with the whole. Thus, an obvious question is: what is the true accuracy of 'standard' discretizations when aiming at computing hyperbolic systems with source terms, especially when highly unsteady patterns travel through the interface between these codes? An elementary investigation has been performed, considering the same set of equations on both sides of the interface, while focusing on two rather classical classes: (i) fractional step methods FSMs), which treat separately convection and sources and (ii) well-balanced schemes ([56], noted WBS afterwards) which have been designed to get accurate approximations of steady states on coarse meshes. This work is discussed in detail in [57], where the model problem is

$$\frac{\partial \rho}{\partial t} + \frac{\partial (\rho U)}{\partial x} = 0 \tag{25}$$

$$\frac{\partial \rho \alpha}{\partial t} + \frac{\partial (\rho \alpha U)}{\partial x} = \rho S(\rho, \alpha, \tau) \tag{26}$$

$$\frac{\partial \rho U}{\partial t} + \frac{\partial (\rho U^2 + P(\rho))}{\partial x} = 0 \tag{27}$$

DOI: 10.1002/fld

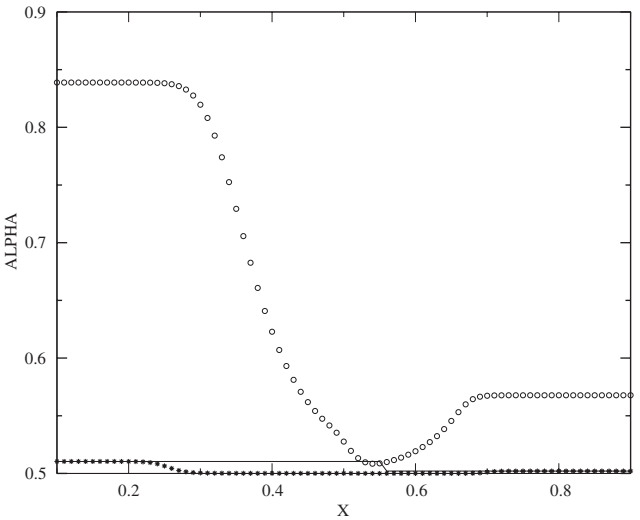

Figure 3. A comparison of the first well-balanced scheme (circles) and the second well-balanced scheme (stars) with the fractional step method (FSM). The mesh contains 100 cells. The relaxation time in the mass transfer term is $\tau = 0.0001$. The parameter $h/U\tau$ is not small compared with 1.

Where ρ, U, α, respectively, stand for the mean density, the mean velocity of the mixture of water and vapour, and the vapour concentration, and $P'(\rho) > 0$. The simple form of the source term $S(\rho, \alpha, \tau)$ which contains a time scale τ which may be tuned, enables to carry on analytical work. In some situations, both explicit schemes FSM and WBS compare quite well, but when the time scale τ becomes too small, results are much in favour of the fractional step approach, even if the latter does not seem to be the ultimate approach.

Results: We show in Figure 3 some computational results which correspond to a Riemann problem including a left-going rarefaction wave and a right-going shock wave. The mesh contains 100 cells. The initial conditions are the following:

$$\begin{aligned} &U(x, t=0) = 10 \\ &\alpha(x<0.5, t=0) = 1 \quad \text{and} \quad \alpha(x>0.5, t=0) = 0.6 \\ &\rho(x<0.5, t=0) = 1 \quad \text{and} \quad \rho(x>0.5, t=0) = 0.5 \end{aligned} \tag{28}$$

It clearly arises here that for this magnitude of $\tau = 10^{-4}$, the FSM performs better than the two different WBS. The solid line in Figure 3 corresponds to the FSM, the circles refer to the standard WBS [56], and the stars correspond to the modified WBS which takes benefit from the particular form of the governing equations (see [57]). The solid line is here indeed close to the exact solution which reads:

$$\begin{aligned} &\alpha(x, t) = a_L(t) \quad \text{if } x < U_1 t \\ &\alpha(x, t) = a_R(t) \quad \text{if } x > U_1 t \end{aligned} \tag{29}$$

DOI: 10.1002/fld

where U_1 stands for the speed of the contact discontinuity, and where $a_{L,R}(t)$ denotes the solution of the ordinary differential equation:

$$\frac{\partial \alpha}{\partial t} = S(\rho, \alpha, \tau) = \frac{1/2 - \alpha}{\tau}$$

We emphasize that the low Mach number regions contribute to the loss of accuracy. Actually, an important parameter that governs the accuracy of approximations of α for the standard WBS in unsteady situations is $h/(U\tau) = M^{-1}(1+M)(\delta t/\tau)(\mathrm{CFL})^{-1}$. For this test case, this one is actually not small compared with 1 (h and δt refer to the mean mesh size and the time step, respectively, and assuming that the CFL number is close to 1). For the standard WBS, this results in a very poor accuracy on *coarse meshes* such as the one considered here. Of course the three schemes converge towards the right solution when the mesh size vanishes [57].

4.2. Free medium/porous medium

A clearly identified problem occurs when the flow of fluid in a free medium enters a porous region (the porosity will be denoted ε). We must assume that the porous formulation (on the right side for instance) has been fixed. We start first with the set of PDE which corresponds to the isentropic Euler equations in a regular porous region. The flow on the left-hand side is also assumed to be governed by conservative-Euler equations. The problem now is to provide a suitable exchange of information through the interface. One may simply suggest that a meaningful interface model simply is the one on the right-hand side:

$$\frac{\partial \rho\varepsilon}{\partial t} + \frac{\partial(\rho\varepsilon U)}{\partial x} = 0 \tag{30}$$

$$\frac{\partial \rho\varepsilon U}{\partial t} + \frac{\partial(\rho\varepsilon U^2)}{\partial x} + \varepsilon\frac{\partial P(\rho)}{\partial x} = 0 \tag{31}$$

Since the latter enables to retrieve the set on the left-hand side. The whole also guarantees that the mean mass flow rate ($\varepsilon\rho U$) is continuous through the interface, which agrees with physical requirements. The continuity of the second Riemann invariant of the stationary wave is nonetheless much more conjectural. Actually the entropy inequality only suggests that the sign of its variation should be correlated with the sign of the mass flow rate through the interface. Moreover, a drawback immediately appears, since one expects that physical grounds should guide the variation of this second invariant. Eventually, one may wonder whether Riemann solvers will handle the whole process, and what the influence of the path that connects ε on both sides of the interface is.

Some attempts to handle this problem are described in [58]. This work tries to address some of the questions above. It obviously arises that almost any interface and cell scheme will correctly treat small variations of ε, but clearly not ratios of 1–0.05. This approach, which is basically influenced by underlying ideas from [56], provides rather satisfactory results from an engineering point of view, but it still requires improvements. A reasonable requirement is that one should at least be able to prescribe some loss of momentum through the interface (this is currently investigated by the working group [59]).

Results: Figure 4 shows some shock wave coming from the free medium (where it has been formed at $x = 0.4$) and propagating to the right side through the 'coupling' interface located on

DOI: 10.1002/fld

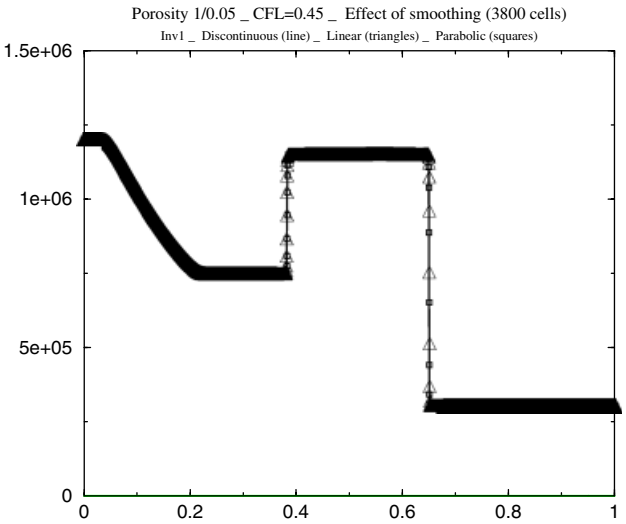

Figure 4. Second steady Riemann invariant $U^2/2+\psi(\rho)$ around the interface between the two codes. The free and porous ($\varepsilon=0.05$) media, respectively, stand on the left and right sides of $x=0.5$. A shock wave is coming from the left and hits this porous interface. Part of the incoming wave is reflected and part is transmitted through the porous medium. The interface approximate Riemann solver, which relies on the VFRoe-ncv approach, enforces the continuity of both steady Riemann invariants. The numerical solution is in agreement with the entropy inequality.

($x=0.5$). The computational domain is [0, 1]. The regular mesh has 3800 cells, and the CFL number is CFL = 0.45. The pressure law is $P(\rho)=10^5\rho^3$. Initial conditions are:

$$\begin{aligned} U(x, t=0) &= 0 \\ \rho(x<0.4, 0) &= 2 \quad \text{and} \quad \rho(x>0.4, 0) = 1 \\ \varepsilon(x<0.5) &= 1 \quad \text{and} \quad \varepsilon(x>0.5) = 0.05 \end{aligned} \tag{32}$$

When the right-going shock wave that has been formed on the left side of the coupling interface hits the coupling interface, a reflected shock wave (which travels to the left) and a transmitted shock wave (which goes to the right) are formed. Through the coupling interface, if we set $\psi(\rho)=\int_0^\rho (P'(a)/a)\,\mathrm{d}a$, we expect that:

$$[\rho\varepsilon U]_-^+ = 0 \tag{33}$$

$$[\rho\varepsilon U(U^2/2+\psi(\rho))]_-^+ \leqslant 0 \tag{34}$$

Though not depicted here, cell values of the mean flow rate $\rho\varepsilon U$ through the coupling interface are correctly represented. The jump of the second invariant $U^2/2+\psi(\rho)$ (see Figure 4) through the interface is in agreement with the overall entropy inequality. Moreover, the approximate solution—on sufficiently fine meshes—does not depend on the interface path, whatever one introduces a discontinuous path (straight line), a linear path (triangles), or a quadratic path—on a given number of cells—(squares) to 'smooth' the interface separating the two codes. Similar test cases involving

DOI: 10.1002/fld

rarefaction waves which hit the interface are discussed in [58], where it is emphasized that many approximate Riemann solvers fail at predicting the above-mentioned expected behaviour.

4.3. Flows through pipes and reactors

The coupling of the 1D CATHARE code with the 3D FLICA IV code requires providing information (boundary conditions in fact) between a 3D code and a 1D code. In order to examine this problem, we have first investigated the coupling of the isentropic Euler set of equations in a 1D and a 2D framework. This has been reported in [60].

More recently, this work has been extended in order to track possible drawbacks when the total energy equation is accounted for. For that purpose, rather than considering a true 3D medium, we have restricted to a 2D framework, which enables us to perform hudge mesh refinements, and thus examine the true drawbacks of coupling strategies, which cannot be afforded when using 3D meshes.

The 2D code thus provides approximations of the following set of PDEs on the right-hand side of the interface (say $x = x_{\text{int}}$):

$$\frac{\partial \rho}{\partial t} + \frac{\partial (\rho U)}{\partial x} + \frac{\partial (\rho V)}{\partial y} = 0 \tag{35}$$

$$\frac{\partial \rho U}{\partial t} + \frac{\partial (\rho U^2 + P)}{\partial x} + \frac{\partial (\rho U V)}{\partial y} = 0 \tag{36}$$

$$\frac{\partial \rho V}{\partial t} + \frac{\partial (\rho U V)}{\partial x} + \frac{\partial (\rho V^2 + P)}{\partial y} = 0 \tag{37}$$

$$\frac{\partial E_2}{\partial t} + \frac{\partial (U(E_2 + P))}{\partial x} + \frac{\partial (V(E_2 + P))}{\partial y} = 0 \tag{38}$$

with the closure law:

$$E_2 = \rho e(P, \rho) + \rho(U^2 + V^2)/2$$

Meanwhile, the 1D code relies on the governing set of equations:

$$\frac{\partial \rho}{\partial t} + \frac{\partial (\rho U)}{\partial x} = 0 \tag{39}$$

$$\frac{\partial \rho U}{\partial t} + \frac{\partial (\rho U^2 + P)}{\partial x} = 0 \tag{40}$$

$$\frac{\partial E_1}{\partial t} + \frac{\partial U(E_1 + P)}{\partial x} = 0 \tag{41}$$

with the EOS:

$$E_1 = \rho e(P, \rho) + \rho U^2/2$$

For convenience, we have restricted to perfect gas EOS, that is: $\rho e(P, \rho) = P/(\gamma - 1)$.

In order to define an interface model, a straightforward idea consists in using the natural candidate corresponding to the projection along the x-axis of the 2D model (35). Nonetheless, it

DOI: 10.1002/fld

immediately appears that the latter one does not comply with the expected and necessary condition $V((x - x_{\text{int}})/t = 0^-) = 0$. Besides, the non-conservative interface model:

$$\frac{\partial Z}{\partial t} = 0 \tag{42}$$

$$\frac{\partial \rho}{\partial t} + \frac{\partial(\rho U_n)}{\partial n} = 0 \tag{43}$$

$$\frac{\partial \rho U_n}{\partial t} + \frac{\partial(\rho U_n^2 + P)}{\partial n} = 0 \tag{44}$$

$$\frac{\partial E_1}{\partial t} + \frac{\partial U_n(E_1 + P)}{\partial n} = 0 \tag{45}$$

$$\frac{\partial U_\tau}{\partial t} + Z U_n \frac{\partial U_\tau}{\partial n} = 0 \tag{46}$$

(with $n = x$, $U_n = U.n$ and $U_\tau = U.\tau$) obeys the different constraints.

Alternatively, one may consider the conservative interface model:

$$\frac{\partial Z}{\partial t} = 0 \tag{47}$$

$$\frac{\partial \rho}{\partial t} + \frac{\partial(\rho U_n)}{\partial n} = 0 \tag{48}$$

$$\frac{\partial \rho U_n}{\partial t} + \frac{\partial(\rho U_n^2 + P)}{\partial n} = 0 \tag{49}$$

$$\frac{\partial E_1}{\partial t} + \frac{\partial U_n(E_1 + P)}{\partial n} = 0 \tag{50}$$

$$\frac{\partial \rho U_\tau}{\partial t} + \frac{\partial Z \rho U_n U_\tau}{\partial n} = 0 \tag{51}$$

One may derive a Godunov scheme for both the non-conservative interface model and the conservative interface model. The exact solution will agree with the constraint: $V((x - x_{\text{int}})/t = 0^-) = 0$. We can also compute approximate solutions of the true 2D solution everywhere in the computational domain while using the 2D code refining the mesh size very much.

Results: The next figure (Figure 5) shows the distribution of transverse momentum in a pipe and a tank, using a 1D code in the pipe that is aligned with the x-axis, and a 2D code in the tank. The coupling interface lies at the junction between the pipe and the tank ($x = 0$). The flow is at rest everywhere at the beginning of the computation. An oblique shock wave, that is formed inside the tank by means of a Riemann data, will hit the coupling interface after a while. The aim of this computation is to maximize the mass flow rate at the coupling interface, and meanwhile to involve great values of the tangential velocity, in order to maximize the 'pollution' around the interface. The whole mesh contains around 40 000 cells. Approximate Godunov solvers are used in both

DOI: 10.1002/fld

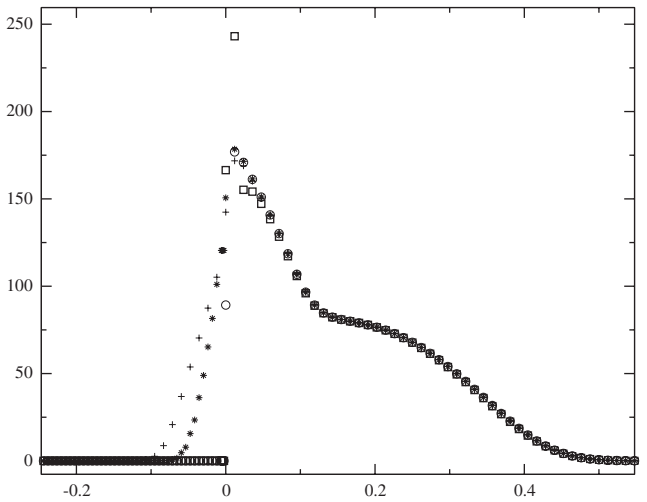

Figure 5. The figure shows the mean y-momentum around the interface between the two codes, along the x-axis aligned with the pipe. The 1D code and the 2D code, respectively, stand on the left and right sides of the coupling interface $x = 0$. They both compute approximations of Euler equations. The oblique shock wave has hit the coupling interface. The comparison includes a computation with the 2D code used throughout the computational domain (crosses), together with the admissible non-conservative coupling model (circles), the admissible conservative coupling model (squares), and the natural conservative model (stars).

codes to discretize equations. The results show a rather good agreement with results associated with a full 2D code, when using the non-conservative approach. The conservative approach leads to a violation of the positivity of the density when the physical time increases.

The paper [60] examines in detail the influence of the EOS (water or vapour), the influence of the coupling model at the interface, the major role of the interface location in the pipe $x = x_{\text{int}}$, and of course the influence of the mesh size.

4.4. Some attempts to couple HEM and HRM models

We also need to investigate the coupling of expected similar models in a 1D framework. Such a case will typically occur when coupling the homogeneous relaxation model (HRM) and a homogeneous equilibrium model (HEM). We detail below some of the recent achievements on that topic.

We start first with the HRM model on the right side of the interface $x > x_{\text{int}}$. For that purpose, we consider that the two phases share the same velocity field U, that is $U_{\text{l}} = U_{\text{v}} = U$, where subscripts l and v, respectively, refer to the liquid phase and the vapour phase. If ρ, P and C denote the density of the mixture, the mean pressure and the liquid mass fraction, a source term $\rho\Gamma(\rho, P, C)$ which involves a positive time scale τ_0 is introduced in order to account for the mass transfer between phases. Hence, the governing equations of the HRM model are:

$$\frac{\partial \rho C}{\partial t} + \frac{\partial \rho C U}{\partial x} = \rho\Gamma(\rho, P, C) \tag{52}$$

DOI: 10.1002/fld

$$\frac{\partial \rho}{\partial t} + \frac{\partial \rho U}{\partial x} = 0 \tag{53}$$

$$\frac{\partial \rho U}{\partial t} + \frac{\partial \rho U^2 + P}{\partial x} = 0 \tag{54}$$

$$\frac{\partial \rho E}{\partial t} + \frac{\partial U(\rho E + P)}{\partial x} = 0 \tag{55}$$

noting:

$$E = e_{\mathrm{HRM}}(P, \rho, C) + \frac{U^2}{2} \quad \text{and} \quad e_{\mathrm{HRM}}(P, \rho, C) = h_{\mathrm{HRM}}(P, \rho, C) - \frac{P}{\rho}$$

It remains to prescribe the closure laws for thermodynamics:

$$\rho h_{\mathrm{HRM}}(P, \rho, C) = \rho C h_{\mathrm{l}}(P, \rho_{\mathrm{l}}) + \rho(1 - C) h_{\mathrm{v}}^s(P) \tag{56}$$

with:

$$\rho_{\mathrm{l}} = \rho C \frac{1}{1 - \rho(1 - C)\tau_{\mathrm{v}}^s(P)} = \frac{C}{\tau - (1 - C)\tau_{\mathrm{v}}^s(P)}$$

The gas is always in a saturation state, and $h_{\mathrm{v}}^s(P)$ and $\tau_{\mathrm{v}}^s(P)$ are given functions. We also assume that the EOS within each pure phase are perfect gas EOS. Thus, the following relations holds:

$$(\gamma - 1)\rho e = P \quad \text{or} \quad h = \delta P \tau \quad \text{with } \delta = \gamma/(\gamma - 1)$$

with $\gamma > 1$.

On the left side of the interface $x < x_{\mathrm{int}}$, the code is assumed to compute approximations of the HEM model, that is:

$$\frac{\partial \rho}{\partial t} + \frac{\partial \rho U}{\partial x} = 0 \tag{57}$$

$$\frac{\partial \rho U}{\partial t} + \frac{\partial \rho U^2 + P}{\partial x} = 0 \tag{58}$$

$$\frac{\partial \rho E}{\partial t} + \frac{\partial U(\rho E + P)}{\partial x} = 0 \tag{59}$$

with

$$E = e_{\mathrm{HEM}}(P, \rho) + \frac{U^2}{2} \quad \text{and} \quad e_{\mathrm{HEM}}(P, \rho) = h_{\mathrm{HEM}}(P, \rho) - \frac{P}{\rho}$$

and

$$h_{\mathrm{HEM}}(P, \rho) = C_{\mathrm{eq}} h_{\mathrm{l}}(P, \rho_{\mathrm{l}}(P, \rho, C_{\mathrm{eq}})) + (1 - C_{\mathrm{eq}}) h_{\mathrm{v}}^s(P)$$

and

$$C_{\mathrm{eq}}(P, \rho) = \frac{\tau_{\mathrm{v}}^s(P) - \tau}{\tau_{\mathrm{v}}^s(P) - \tau_{\mathrm{l}}^s(P)} \tag{60}$$

DOI: 10.1002/fld

Unlike in the previous case, here the coupling method at the interface relies on the use of relaxation techniques such as those described in [54, 61]. This is detailed in Reference [62].

Results: The following test case corresponds to the schematic 1D flow in a nuclear power plant. The length of the pipes is 80 m. It includes a part of the coolant circuit containing the core on the left side of the coupling interface (i.e. $-40<x<0$) where the governing set of equations is the HEM model. The core is located in the interval $[-22, -18]$. The total length of the core is the true core length. The core section is equal to 3.5 m^2. The HRM model is used on the right side of the coupling interface (i.e. $0<x<40$). Before the beginning of the computation, the velocity, density and pressure profiles are uniform and equal to: $U = 10\,\mathrm{m\,s^{-1}}$, $\rho = 700\,\mathrm{kg\,m^{-3}}$, $P = 150 \times 10^5$ Pa. Moreover, we initialize $C = C_{\mathrm{eq}}(P, \rho)$ in the HRM part of the coolant circuit. The heat source is null outside the core, and we prescribe:

$$\int_{x=-22}^{x=-18} \Phi(x)\,\mathrm{d}x = \Phi_0 = 3000 \times 10^6\ \mathrm{W}$$

inside the core region. The uniform mesh contains 500 nodes. The governing set of equations in the left part is the set of equations of the HEM model with an equation for the total energy which takes into account the heat source:

$$\frac{\partial \rho E}{\partial t} + \frac{\partial U(\rho E + P)}{\partial x} = \Phi(x)$$

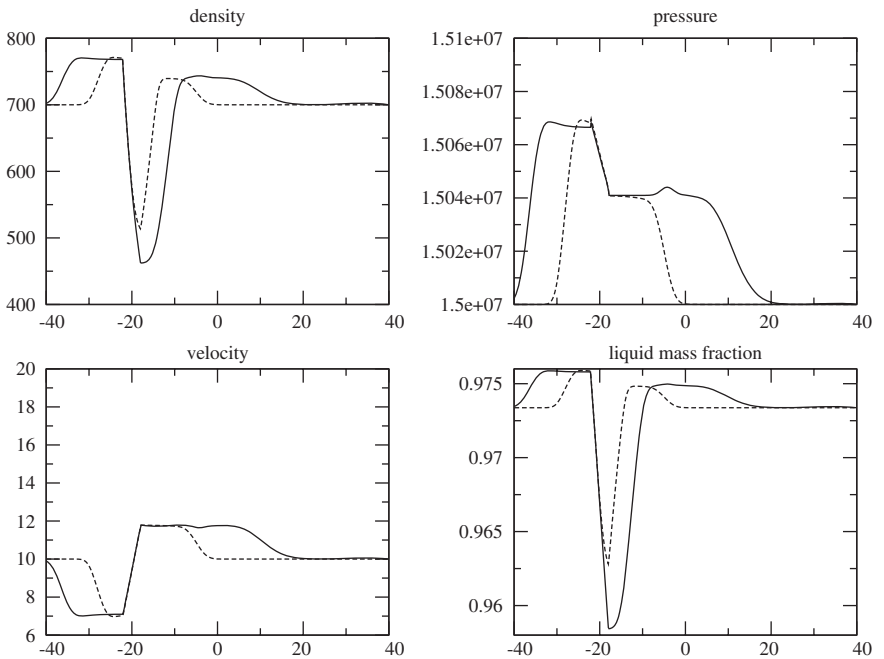

Figure 6. The right-going shock wave before and after its interaction with the coupling interface $x = 0$. Core region: $-22<x<-18$, HEM code: $x<0$, HRM code: $x>0$.

DOI: 10.1002/fld

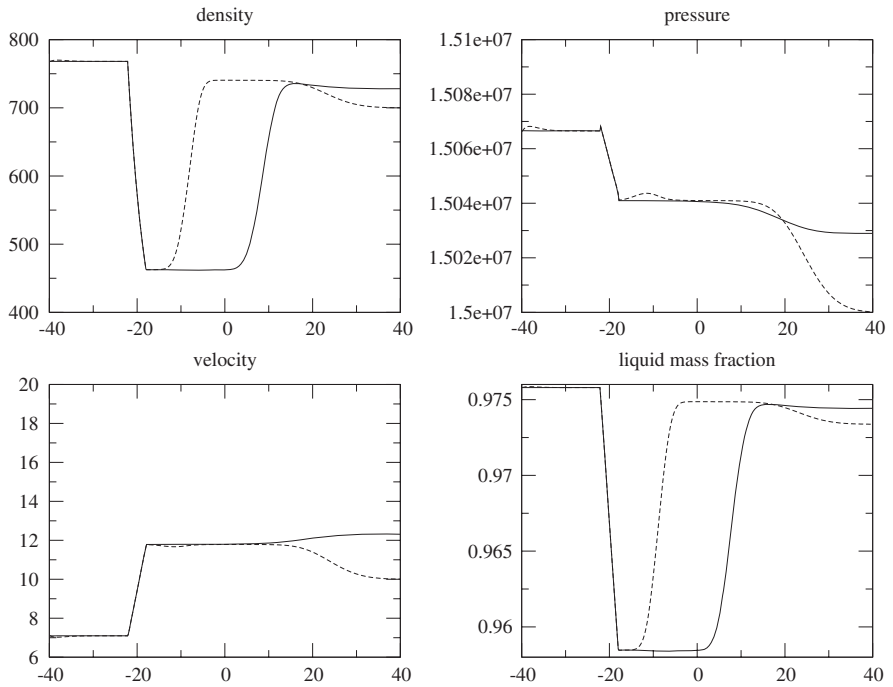

Figure 7. The right-going contact wave before and after its interaction with the coupling interface $x = 0$. Core region: $-22 < x < -18$, HEM code: $x < 0$, HRM code: $x > 0$.

Results have been plotted at four distinct instants.

- At $t = T_1$, the right shock wave, which is coming from the right side of the core, and which is due to the sudden heating in the core region, has not hit the coupling interface yet (dashed line in Figure 6).
- At $t = T_2$, the same right shock wave has already moved through the coupling interface (plain line in Figure 6). One can easily observe at $t = T_2$ the reflected wave in the interval $[-0.25, 0]$, either focusing on the pressure profile, the density profile or the velocity profile. The amplitude of this reflected wave is small compared with the one of the associated shock wave.
- At $t = T_3$, the right-going contact wave has still not passed the coupling interface (dashed line in Figure 7). This contact wave is of course characterized by locally uniform pressure and velocity profiles. At that time, the right-going shock wave has not reached the right exit. The behaviour of the coupling interface seems almost perfect: both the HEM code and the HRM code maintain travelling contact waves (see [14]); moreover, these waves are correctly transmitted from the HEM domain to the HRM domain by the coupling method (see [61]).
- At $t = T_4$, the contact wave is on the right side of $(x = 0)$ (plain line in Figure 7). Once again, everything seems correct around the coupling interface $(x = 0)$. At that time $t = T_4$, the right-going shock wave has gone outside the computational domain. One can of course note

DOI: 10.1002/fld

the influence of the right exit boundary which generates a reflected wave in the computational domain. This is due to the fact that crude Neumann-type boundary conditions have been imposed in this test case.

The impact of discrepancies in EOS formulations or tabulations is also a major problem, since very small variations on thermodynamical coefficients may greatly change results. Actually almost all thermodynamical approaches implemented in industrial codes differ. A straightforward consequence is that the interfacial coupling of codes involving different EOS may pollute the whole solution. The behaviour of expected similar EOS with arbitrary jumps of coefficients, has been examined and reported in [52], where authors take advantage of relaxation techniques to avoid the resonance phenomena which may occur when applying straightforwardly basic ideas relying on the upwinding of source terms for steady situations.

5. CONCLUSION

We made a brief review of NEPTUNE project numerical investigations in this paper, while focusing on two items:

- recent advances in mechanical and numerical modelling of multi-phase flows;
- the interfacial coupling of unsteady codes with distinct models.

Actually, the latter points are far from being mature of course, and some of the problems arising within the second framework confirm that there is still a lot of work to do in order to improve predictions of multi-phase flows, whenever one considers academic or industrial applications. We tried herein to emphasize some possible weaknesses, and also focused on possible alternative strategies in order to improve our understanding of two-phase flow models. Another research direction, which is currently under investigation, concerns the local coupling of models and the hybridization of two-phase flow models.

Owing to current research efforts, it urges for a better synergism between workers in the field, keeping in mind the *objective* fact that computer performances will still go increasing within the next years to come. One should also be aware that we need to propose new approaches and focus on strategies which make sense on the continuous level. This should be achieved with a closer collaboration between mechanicians and applied mathematicians, and European initiatives such as [63] should be greatly encouraged.

ACKNOWLEDGEMENTS

The NEPTUNE project is mainly funded by EDF (Electricité de France) and CEA (Commissariat à l'Energie Atomique), with a complementary support by IRSN (Institut de Radioprotection et Sureté Nucléaire) and AREVA-NP. The main contributors to the work package on numerical methods are: Annalisa Ambroso, Michel Belliard, Philippe Emonot, Samuel Kokh and Anela Kumbaro from CEA. The whole work benefits from contributions of PhD students: Thomas Fortin, Vincent Guillemaud, Olivier Hurisse and Isabelle Ramière. Grégoire Allaire, Philippe Angot, Christophe Chalons, Frédéric Coquel, Thierry Gallouet, Edwige Godlewski, F. Lagoutière, Pierre-Arnaud Raviart and Nicolas Seguin are also acknowledged for their kind support and advice. The authors are indebted to Annalisa Ambroso (CEA), Thierry Gallouet (Université Aix Marseille I), Antoine Guelfi (NEPTUNE project manager, EDF) and Olivier Marchand (EDF) who helped in improving the draft of the manuscript.

DOI: 10.1002/fld

REFERENCES

1. Guelfi A, Bestion D, Boucker M, Boudier P, Fillion P, Grandotto M, Hérard JM, Hervieu E, Peturaud P. NEPTUNE : a new software platform for advanced nuclear thermohydraulics. *Nuclear Science and Engineering* 2005, in press.
2. Bestion D, Guelfi A. Multiscale analysis of thermal hydraulics of nuclear reactors: the NEPTUNE project. *SHF Meeting on Advances in the Modelling Methodologies of Two-phase Flows*, vol. 5, Lyon, France, 24–26 November 2005, La Houille Blanche.
3. Peturaud O, Hervieu E. Physical validation issue of the NEPTUNE two-phase modelling: validation plan to be adopted, experimental programs to be set up and associated instrumentation techniques developed. *SHF Meeting on Advances in the Modelling Methodologies of Two-phase Flows*, Lyon, France, 24–26 November 2004, La Houille Blanche, in press.
4. Eymard R, Gallouet T, Herbin R. Finite volume methods. *Handbook for Numerical Analysis*, Ciarlet PG, Lions PLL (eds), vol. VII, 2001.
5. Allaire G, Clerc S, Kokh S. A five equation model for the simulation of interfaces between compressible fluids. *Journal of Computational Physics* 2002; **181**:577–616.
6. Barberon T, Helluy P. Finite volume simulation of cavitating flows. *Computers and Fluids* 2005; **34**:832–858.
7. Caro F, Coquel F, Jamet D, Kokh S. DINMOD: a diffusive interface model for two phase flow modelling. *IRMA Series in Mathematics and Theoretical Physics* 2004.
8. Caro F, Coquel F, Jamet D, Kokh S. A simple finite volume method for compressible isothermal two-phase flow simulation. *International Journal of Finite Volumes* 2006; **3**(1):1–37 (http://averoes.math.univ-paris13.fr/IJFV/).
9. Guillard H, Muronne A. On the behaviour of upwind schemes in the low Mach number limit: II. Godunov type schemes. *Computers and Fluids* 2004; **33**:655–675.
10. Caro F. *Ph.D. Thesis*, Modélisation et simulation numérique des transitions de phase liquide-vapeur, Ecole Polytechnique, Paris, France, 24 November 2004.
11. Ghidaglia JM, Kumbaro A, Le Coq G. On the numerical simulation to two fluid models via a cell center finite volume method. *European Journal of Mechanics Fluids*, *Series B* 2001; **20**:841–867.
12. Kumbaro A. Simulation of two-phase flows using a multi-size group model. *Third International Symposium on Two Phase Flow Modelling and Experiments*, Pisa, Italy, 2004.
13. Ndjinga M. *Ph.D. Thesis*, Ecole Centrale de Paris, Paris, France, 2006, in preparation.
14. Gallouet T, Hérard JM, Seguin N. A hybrid scheme to compute contact discontinuities in one dimensional Euler systems. *Mathematical Models and Numerical Analysis* 2003; **36**:1133–1159.
15. Guillard H, Muronne A. A five equation reduced model for compressible two phase flow problems. *INRIA Report 4778*, 2003; *Journal of Computational Physics*.
16. Belliard M, Grandotto M. Computation of two phase flow in steam generator using domain decomposition method. *Nuclear Engineering and Design* 2002; **213**:223–239.
17. Belliard M, Grandotto M. Multigrid preconditioning of the steam generator two phase mixture balance equations in the GENEPI software. *Proceedings of NURETH10*, 2003.
18. Belliard M, Grandotto M. Local zoom computation of two phase flows in steam generators using a local defect correction method. *Numerical Heat and Mass Transfer* 2003; **43**:1–5.
19. Fortin T. Une méthode élements finis à décomposition L2 d'ordre élevé motivée par la simulation d'écoulements diphasiques bas Mach. *Ph.D. Thesis*, Université Paris VI, Paris, France, 5 May 2006.
20. Emonot P, Heib S. Convergence of a new nonconforming equal order finite volume element method for the Stokes problem. *SIAM Journal on Scientific Computing* 2002.
21. Angot P, Bruneau CH, Fabrie P. A penalization method to take into account obstacle in incompressible viscous flows. *Numerische Mathematik* 1999; **81**:497–520.
22. Angot P, Lomenede H, Ramière I. A general fictitious domain method with non-conforming structured mesh. *Proceedings of FVCA4*, 2005; 261–272.
23. Belliard M. Using a fictitious domain approach for the numerical modelling of two phase flows in nuclear power plant components. *Proceedings of Supercomputing for Nuclear Applications*, *SNA2003*, 2003.
24. Ramière I, Belliard M, Angot P. On the simulation of nuclear power plant components using a fictitious domain approach. *Proceedings of NURETH11*, 2005.
25. Ramière I, Angot P, Belliard M. A fictitious domain approach with spread interface for elliptic problems with general boundary conditions. *Computer Methods in Applied Mechanics and Engineering* 2007; **196**:766–781.

DOI: 10.1002/fld

26. Ramière I. Méthodes de domaines fictifs pour des problèmes elliptiques avec conditions aux limites générales en vue de la simulation numérique d'écoulements diphasiques. *Ph.D. Thesis*, Université Aix Marseille I, Marseille, France, 2006.
27. Perron S. Résolution de problèmes d'écoulements thermiques en 3D avec une nouvelle méthode de Volumes Finis. *Ph.D. Thesis*, Université du Québec à Chicoutimi, Québec, Canada, 15 November 2001.
28. Coquel F, El Amine K, Godlewski E, Rascle P, Perthame B. A numerical method using upwind schemes for the resolution of twophase flows. *Journal of Computational Physics* 1998; **136**:272–288.
29. Hérard JM, Hurisse O. A relaxation method to compute two-fluid models. *International Journal of Computational Fluid Dynamics* 2004; **19**(7):475–482.
30. Baer MR, Nunziato JW. A two phase mixture theory for the deflagration to detonation transition (DDT) in reactive granular materials. *International Journal of Multiphase Flow* 1986; **12**(6):861–889.
31. Kapila AK, Son SF, Bdzil JB, Menikoff R, Stewart DS. Two phase modelling of DDT: structure of the velocity relaxation zone. *Physics of Fluids* 1997; **9**(12):3885–3897.
32. Gavrilyuk S, Gouin H, Perepechko YV. A variational principle for two-fluid models. *Comptes Rendus de l Academie des Sciences*, *Paris IIb* 1997; **324**:483–490.
33. Gavrilyuk S, Gouin H. A new form of governing equations of fluids arising from Hamilton's principle. *International Journal of Engineering Science* 1999; **37**:1495–1520.
34. Gallouet T, Hérard JM, Seguin N. Numerical modelling of two phase flows using the two-fluid two-pressure approach. *Mathematical Models and Methods in Applied Sciences* 2004; **14**:663–700.
35. Gavrilyuk S, Saurel R. Mathematical and numerical modelling of two phase compressible flows with micro-inertia. *Journal of Computational Physics* 2002; **175**:326–360.
36. Gavrilyuk S. Acoustic properties of a two-fluid compressible mixture with micro inertia. *European Journal of Mechanics*, *Series B* 2005; **24**:397–406.
37. Hérard JM. A turbulent hyperbolic two-phase flow model. 2005, submitted.
38. Schwendeman DW, Wahle CW, Kapila AK. The Riemann problem and high resolution Godunov method for a model of compressible two-phase flow. *Journal of Computational Physics* 2006; **212**:490–526.
39. Buffard T, Gallouet T, Herard JM. A sequel to a rough Godunov scheme. Application to real gases. *Computers and Fluids* 2000; **29**(7):813–847.
40. Castro CE, Toro EF. A Riemann solver and upwind methods for a two-phase flow model in nonconservative form. *International Journal for Numerical Methods in Fluids* 2006; **50**:275–307.
41. Guillemaud V. *Ph.D. Thesis*, Université Aix-Marseille I, 2006, in preparation.
42. Coquel F, Perthame B. Relaxation of energy and approximate Riemann solvers for general pressure laws in fluid dynamics. *SIAM Journal on Numerical Analysis* 1998; **35**:2223–2249.
43. Baudin N, Berthon C, Coquel P, Masson R, Tran H. A relaxation method for two phase flow models with hydrodynamic closure law. *Numerische Mathematik* 2005; **99**(3):411–430.
44. Helluy P. Simulation numérique des écoulements multiphasiques: de la théorie aux applications. Toulon, 2005, (http://helluy.univ-tln.fr/ADMIN/habilitation.pdf).
45. Nussbaum J. *Ph.D. Thesis*, Université de Toulon, 2007, in preparation.
46. Hérard JM. An hyperbolic three-phase flow model. *Comptes Rendus de l Academie des Sciences*, *Paris I* 2006; **342**:779–784.
47. Coquel F, Gallouet T, Hérard JM, Seguin N. Closure laws for two-fluid two-pressure models. *Comptes Rendus de l Academie des Sciences*, *Paris I* 2002; **334**:927–932.
48. Hérard JM. A three-phase flow model. *EDF Report HI-81/04/11/A*; *Mathematical and Computer Modelling* 2007; **45**:732–755.
49. Ambroso A. An introduction to the problem of interfacial coupling of thermohydraulic models. *Internal CEA Report SFME/LETR/04-008/A*, 2004,
50. Godlewski E, Raviart PA. The numerical coupling of non-linear hyperbolic systems of conservation laws. I: The scalar case. *Numerische Mathematik* 2004; **97**:81–130.
51. Godlewski E, Le Thanh K, Raviart PA. The numerical coupling of non-linear hyperbolic systems of conservation laws. II: The case of systems. *Mathematical Models and Numerical Analysis* 2005; **39**:649–692.
52. Ambroso A, Chalons C, Coquel F, Godlewski E, Lagoutière F, Raviart PA, Seguin N, Hérard JM. Coupling of multiphase flow models. *Proceedings of NURETH11*, Aix en Provence, Popes' Palace, 2005.
53. Ambroso A, Chalons C, Coquel F, Godlewski E, Lagoutière F, Raviart PA, Seguin N. Homogeneous models with phase transition: coupling by finite volume methods. *Proceedings of FVCA4*, 2005; 483–492.

DOI: 10.1002/fld

54. Ambroso A, Chalons C, Coquel F, Godlewski E, Lagoutière F, Raviart PA, Seguin N. The coupling of homogeneous models for two-phase flows. *International Journal of Finite Volumes*, in press. http://averoes.math.univ-paris13.fr/IJFV/
55. Hérard JM, Hurisse O. Couplage interfacial instationnaire d'un modèle homogène et d 'un modèle bifluide. *Internal EDF Report H-I81-2006-04691-FR*, in press.
56. Greenberg JM, Le Roux AY. A well balanced scheme for the numerical processing of source terms in hyperbolic equations. *SIAM Journal on Numerical Analysis* 1996; **33**(1):1–16.
57. Gallouet T, Hérard JM, Hurisse O, Le Roux AY. Well balanced schemes versus fractional step method for hyperbolic systems with source terms. *Calcolo* 2005, in press.
58. Hérard JM. Naive schemes to compute isentropic flows between free and porous medium. *EDF Report HI-81/04/08/A*; *International Journal of Finite Volumes* 2004; **3**(2):1–28 (http://averoes.math.univ-paris13.fr/IJFV/).
59. Ambroso A, Chalons C, Coquel F, Godlewski E, Lagoutière F, Raviart PA, Seguin N. Joint CEA-SFME/Laboratoire Jacques-Louis Lions Working Group on the Coupling of Models in Thermal Hydraulics.
60. Hérard JM, Hurisse O. Coupling two and one-dimensional unsteady Euler equations through a thin interface. *Computers and Fluids* 2007; **36**.
61. Hurisse O. Couplage interfacial instationnaire de modèles diphasiques. *Ph.D. Thesis*, Université Aix Marseille I, Marseille, France, 16 October 2006.
62. Hérard JM, Hurisse O. A method to couple HEM and HRM two-phase flow models. *EDF Report HI-81/06/01/A* 2006, submitted.
63. DFG-CNRS Working Group FOR 563. Micro–macro modeling and simulation of liquid vapour flows. 2005. http://www.mathematik.uni-freiburg.de/IAM/dfg-cnrs/

DOI: 10.1002/fld